Comparison of alternative algorithms for buckling analysis of slender steel structures

C.A. Dimopoulos* and C.J. Gantes[a]

Institute of Steel Structures, School of Civil Engineering, National Technical University of Athens, Greece

Abstract. Objective of this paper is to compare linear buckling analysis formulations, available in commercial finite element programs. Modern steel design codes, including Eurocode 3, make abundant use of linear buckling loads for calculation of slenderness, and of linear buckling modes, used as shapes of imperfections for nonlinear analyses. Experience has shown that the buckling mode shapes and the magnitude of buckling loads may differ, sometimes significantly, from one algorithm to another. Thus, three characteristic examples have been used in order to assess the linear buckling formulations available in the finite element programs ADINA and ABAQUS. Useful conclusions are drawn for selecting the appropriate algorithm and the proper reference load in order to obtain either the classical linear buckling load or a good approximation of the actual geometrically nonlinear buckling load.

Keywords: buckling analysis; steel structures; column; arch; shell; nonlinear behaviour

1. Introduction

In recent years structural design codes have adopted limit state design (LSD) replacing the older concept of allowable stress design (ASD) (European Committee for Standardisation 2004a, American Institute of Steel Construction 1999). In ASD the focus is on keeping the stresses due to design loads below a certain working stress level. In contrast to ASD, LSD is based on a more realistic determination of the strength capacity of the structure. This capacity is obtained either by code regulations based mostly on experimental results or by sophisticated finite element analyses with appropriate modelling regarding the material properties, the initial imperfections, the initial stresses and the boundary conditions. Limit state design requires the structure to satisfy two principle criteria: the ultimate limit state (ULS) and the serviceability limit state (SLS). The ultimate limit state is satisfied if the load-carrying capacity of the structure is sufficiently large for all possible pertinent load combinations described by the codes, while the serviceability limit state (SLS) is satisfied if under routine, everyday loading the structure maintains its functionality.

In Limit State Design, a key point is the accurate determination of the collapse load of the structure. Phenomena like local buckling and component deterioration in strength and/or stiffness due to cumulative plastic strains at various locations (Lignos *et al*. 2011), could lead the structure

*Corresponding author, Ph.D., E-mail: dchristoforos@hotmail.com
[a]Professor, E-mail: chgantes@central.ntua.gr

into collapse. In general, collapse can be primarily due to material nonlinearity or geometric nonlinearity or a combination of the two. The magnitude of the global and local slenderness determines whether a structure can be characterized as stocky, in which case material nonlinearity prevails, or slender, in which case geometric nonlinearity is dominant. For example, the slenderness of beam-column members depends on the ratio of their length to the radius of inertia of their cross-section; the slenderness of plane members is associated to the ratio of their in-plane dimensions to their thickness. According to Parts 1.1 and 1.6 of Eurocode 3 (European Committee for Standardization 2004a, European Committee for Standardization 2006) columns or cylindrical shells under axial compression with slenderness values smaller than 0.2 are not affected by buckling and can thus be characterized as stocky. Stocky structures collapse when material yielding takes place in a sufficient number of cross-sections that would turn the structure into a mechanism. Very slender structures fail under instability phenomena associated with large increase of deformation for a small increase in applied load, a condition known as geometric nonlinearity. Structures of intermediate slenderness collapse under a combination of the two aforementioned sources of nonlinearity, as is practically always the case for building structures.

The prevailing design method recommended by pertinent codes, including Eurocode 3 (European Committee for Standardisation 2004a), is the determination of the member actions by means of linear elastic analyses of the structure subjected to the design loads. The member actions are then compared with the member resistance that take into account both types of nonlinearity. A common methodology that is adopted by the codes for the determination of the member resistance is the application of reduction factors on the plastic capacity of the member's cross-section (Sedlacek and Müller 2006). In order to do that, knowledge of the member's slenderness is necessary.

The use of a linear elastic analysis for strength verification is a significant advantage for practical applications since it is simple and straightforward, can be carried out by means of widely available commercial software, is computationally inexpensive and requires relatively small effort on behalf of the engineer in setting up the model and interpreting the results. Furthermore, the results are quite reliable for ordinary structural systems, consisting of members with normal profile cross-sections as well as built-up cross-sections (Johansson *et al.* 2001).

Uncommon structural systems, such as structures supporting free-form architecture or shells with cut-outs, and members that are curved in space and have unusual cross-sections, are not covered by provisions in design codes, so that the use of existing reduction factors may not be suitable. In such cases, appropriate nonlinear finite element analyses can be used to predict the collapse load, as also allowed by modern codes (European Committee for Standardization 2004a, American Institute of Steel Construction 1999, European Committee for Standardization 2004b, European Committee for Standardization 2006). Depending on the type of loading, the collapse load coefficient is determined which, when multiplied with the design loading applied on the structure, results in zero stiffness, corresponding to the maximum point on a characteristic load-displacement curve. When applying these codes, practicing engineers must have sufficient guidelines for setting up numerical models, selecting proper analysis methods and numerical algorithm parameters and interpreting the results. Recent technical literature contributes in that direction (Chen and Kim 1997, Kim *et al.* 2001, Paik and Thayamballi 2003, Agüero and Pallarés 2007, among others).

Exploitation of the capabilities of computational tools for obtaining the ultimate strength has been investigated by a large number of researches for a variety of structural types. A large part of this effort was directed towards frame structures (e.g., Hsieh and Deierlein 1991, Liew *et al.* 1993, 2000, White 1993, Pi and Trahair 1994a, b, Chan and Chui 2000, White and Hajjar 2000, Kim *et*

al. 2001). Several other applications have also been addressed by investigators, such as tubular structures (Chan 1989), transmission towers (Al-Bermani and Kitipornchai 1992), space trusses (Yang *et al*. 1997), reticulated domes (Kato *et al*. 1998), storage pallet racks (Baldassino and Bernuzzi 2000), frames with out-of-plane effects (Trahair and Chan 2003), arches (Pi and Bradford 2004, Dimopoulos and Gantes 2008a, b) and offshore steel jacket structures (Rodrigues and Jacob 2005). Furthermore, thin-walled, plated and shell structures have also been investigated (Al-Bermani and Kitipornchai 1990, Shanmugam *et al*. 1993, Elgaaly 2000, Gettel and Schneider 2007). Validation of numerically obtained collapse loads against experimental data is always recommended for increased reliability of numerical results (e.g., Shi *et al*. 2012, Hawileh *et al*. 2012).

A systematic methodology for predicting collapse of steel structures by means of nonlinear numerical analysis, making use of commercially available finite element software, has been proposed in (Gantes and Fragkopoulos 2010). This strategy consists of setting up an appropriate finite element model, obtaining critical buckling modes from linearized buckling analysis (LBA), and then using a linear combination of these modes as imperfection pattern for a geometrically and material nonlinear imperfection analysis (GMNIA). Equilibrium paths accompanied by snapshots of deformation and stress distribution at characteristic points are proposed as a powerful tool for evaluating the results of the GMNI analysis. Thus, the static collapse load of a wide variety of structures can be evaluated. In the case of dynamical systems (e.g., structures under seismic loading), this methodology should be adapted accordingly to include the dynamic nature of loading.

The engineers applying the proposed methodology should have good knowledge of theoretical and practical aspects of the finite element method for linear and nonlinear structural applications, as outlined, for example, in (Bathe and Cimento 1980, Bathe *et al*. 1980, Bathe 1995, Crisfield *et al*. 1997, Kojic and Bathe 2004). The geometric and material nonlinear phenomena characterizing steel structures near collapse are very complicated in nature and require, in most cases, highly sophisticated numerical tools for their simulation. The simplest numerical method for a detailed geometrically and material nonlinear (GMN) analysis is the Newton-Raphson scheme (Bathe 1995), which can be found in three forms: (i) the full Newton-Raphson, which is the most accurate, but also the most time consuming, since the tangent stiffness of the structure has to be calculated and factorized within each iteration in the solution procedure, (ii) the modified Newton-Raphson, which differs from the full Newton-Raphson in that the calculation and the factorization of the tangent stiffness matrix takes place only in some iterations within each step, thus requiring in most cases a larger number of iterations per step but a smaller computational effort per iteration, and (iii) the 'initial stress' Newton-Raphson procedure, where the calculation of the tangent stiffness matrix is performed once, at the beginning of the analysis, and then kept the same during the analysis.

Applying the Newton-Raphson method in a nonlinear finite element system will yield results only in the pre-collapse range, but it will fail to give information about the post-collapse range. To circumvent this limitation, a constraint can be added into the finite element system, which relates the load increment and the incremental displacements within each iteration. This technique allows the calculation of the whole equilibrium path, even beyond the critical limit points. A number of different solution algorithms have been proposed in the literature (Riks 1979, Crisfield 1981, Ramm 1981, Bathe and Dvorkin 1983). Even with this modification of the finite element system, the direct computation of bifurcation points cannot be achieved and the calculation of limit points is not 'exact'. However, this can be achieved by simply introducing an additional constraint in the finite element system, which concerns the different stability conditions of the bifurcation and the limit points (Wriggers and Simo 1990, Wriggers *et al*. 1987).

Critical buckling loads obtained by means of linearized buckling analyses (LBA) (Bathe 1995) are, in most cases, not safe predictions of strength. However, this type of analysis must always precede the subsequent, more exact, nonlinear analyses, for several reasons: (i) Critical buckling loads obtained by means of linearized buckling analyses are an initial indication, and in most cases an upper bound, of actual strength. Taking also into account the fact that this is a very fast and inexpensive type of analysis, it may be very useful as a tool for evaluating alternative solutions during preliminary design, before resorting to the much more time-consuming and expensive nonlinear analyses. (ii) Critical buckling loads are often needed for calculating non-dimensional slenderness ratios to be used with buckling curves in the framework of code-based design procedures. Even though analytical expressions for these buckling loads are available for simple cases of geometry, loading patterns and boundary conditions, in the majority of other cases buckling loads must be obtained numerically. (iii) It has been shown that buckling analysis can be used in place of a geometrically nonlinear analysis for the calculation of the nonlinear stability limit of a number of structures by performing a number of successive buckling analyses on the unstressed and some stressed configurations of the structures (Chang and Chen 1986). (iv) Buckling modes obtained by means of linearized buckling analyses are commonly used as initial imperfections for geometrically and material nonlinear imperfection analyses (GMNIA). Such imperfections are necessary in order to trigger all possible failure mechanisms and to make sure that the critical failure mechanism is captured by the numerical analysis algorithm.

It should be noted that the choice of buckling modes as imperfection patterns is not unique, and has in many cases been found to lead to lower compliance to experimental results than other shapes of initial imperfections. For the case of cylindrical shell structures, a type of structures that is particularly sensitive to imperfections, it has been demonstrated (Schneider and Brede 2005, Schneider *et al.* 2005) that different patterns can be decisive depending on the imperfection amplitude and that these amplitude-depending patterns cannot be determined with certainty because of the considerable influence of material nonlinearity and because of the numerous post-buckling paths which cross each other. Imperfections affine to the collapse mode of the perfect shell were found to be more unfavourable than ideal buckling modes. In column members depending on the member slenderness and the cross-section properties, either global flexural or local imperfections must be taken into account, or even a combination of both types of imperfection, in order for the nonlinear finite element analyses to capture the lowest possible collapse load (see for example Kaitila 2002, Feng *et al.* 2004).

Furthermore, fabrication processes are responsible for imperfection patterns, creating residual stress profiles in the body of the cross-sections, which can have significant consequences on the ultimate bearing capacity of steel structures (Berry *et al.* 2000, Herynk *et al.* 2007). However, the choice of manufacturing-related imperfection patterns is usually dependent upon the structural type as well as the specific manufacturing method, can not be easily generalized, and often lacks adequate data to be properly implemented. In case such information is available, it is, in general, preferable to use these imperfection patterns, as they more accurately represent real strength. In the absence of such data, however, the use of buckling modes as imperfection shapes is considered to be the next best available choice. As far as the effect of the residual stresses on the strength of steel structures is concerned, it has been found to be more significant on moderate slenderness structures (e.g., beams and arches under lateral-torsional buckling) instead of the stockier or very slender structures (Pi and Trahair 1998, Pi *et al.* 1999, Vila Real *et al.* 2004). Even the type of loading could affect the influence of residual stresses on the strength of the structures (Pi and Trahair 1998).

As stated also in all relevant design codes that allow use of advanced analysis to evaluate collapse loads (European Committee for Standardization 2004a, American Institute of Steel Construction 1999, European Committee for Standardization 2004b, European Committee for Standardization 2006), it should be verified that the eigenvalue algorithm that is used is reliable in finding the eigenmode that leads to the lowest eigenvalue. This issue has already been identified and discussed by Earls (2007). Therefore, it is crucial to have a good knowledge of the buckling analysis algorithms that are available in commercial finite element software and can be thus encountered in practice. Objective of this paper is to describe several buckling analysis algorithms that are implemented in such software, and to make proposals for appropriate selection of algorithms and parameters, depending on the purpose of the analysis.

To that effect, the basic equations of the geometrically nonlinear finite element formulation are briefly mentioned, and the necessary simplifications for obtaining the linear buckling equations are made. The specific linear buckling algorithms used in ADINA (2006) and ABAQUS (2008) are presented, and then they are used for analyzing three examples, each typical of a different type of nonlinear behaviour. The results are generalized in order to draw conclusions and propose guidelines for the appropriate implementation of each algorithm in practice.

It is emphasized that the above analysis methods are well known in the academic structural engineering community, thus the contribution of the present work is not geared towards the methods themselves. On the other hand, the majority of practicing structural engineers is not familiar with strength evaluation using advanced analysis techniques. Thus, the aim of this work is to contribute towards closing this gap, by providing practical guidelines for using advanced analysis for structural design, and by demonstrating some of the capabilities afforded to structural engineers by such methods.

2. Nonlinear finite element formulation

To understand the basic principles behind linear or linearized buckling analysis, some information should be given first regarding nonlinear analysis in the context of the finite element method. Consider the motion of a general body in a stationary Cartesian coordinate system that experiences large displacements, large strains and a linear or nonlinear constitutive response. It is supposed that the solutions for the static and kinematic variables are known from time 0 (initial configuration) up to the time t. Then, the solution at the next required equilibrium position corresponding to time $t + \Delta t$ is sought. According to Bathe (1995), in the large displacement formulation, the equilibrium condition can be expressed, using the principle of virtual displacements, with the equation

$$\int_{^0V} {}^{t+\Delta t}_{0}\mathbf{S}_{ij} \, \delta \, {}^{t+\Delta t}_{0}\varepsilon_{ij} d^0V = {}^{t+\Delta t}\mathbf{R} \tag{1}$$

where ${}^{t+\Delta t}_{0}\mathbf{S}_{ij}$ is the second Piola-Kirchhoff stress tensor

$$ {}^{t+\Delta t}_{0}\mathbf{S}_{ij} = \frac{{}^{0}\rho}{{}^{t+\Delta t}\rho} \, {}^{0}_{t+\Delta t}\mathbf{x}_{i,m} \, {}^{t+\Delta t}\tau_{mn} \, {}^{t+\Delta t}_{0}\mathbf{x}_{j,n} \tag{2}$$

and ${}^{t+\Delta t}_{0}\varepsilon_{ij}$ is the Green-Lagrange strain tensor

$$\delta^{t+\Delta t}_0\varepsilon = \delta\frac{1}{2}(^{t+\Delta t}_0\mathbf{u}_{i,j} + {}^{t+\Delta t}_0\mathbf{u}_{j,i} + {}^{t+\Delta t}_0\mathbf{u}_{k,i}{}^{t+\Delta t}_0\mathbf{u}_{k,j}) \tag{3}$$

while $^{t+\Delta t}\mathbf{R}$ corresponds to the externally applied loads at time $t+\Delta t$, $^{t+\Delta t}\tau_{mn}$ are the Cartesian components of the Cauchy stress tensor in the deformed geometry at time $t+\Delta t$, $^{t+\Delta t}_0\mathbf{x}_i$ denotes the Cartesian coordinates of material point at time $t+\Delta t$, $^{t+\Delta t}\rho$ is the mass density of the body at time $t+\Delta t$ and $^{t+\Delta t}_0\mathbf{u}_i$ are the components of the displacement vector at the configuration at time $t+\Delta t$.

In the above quantities, the terminology of Bathe (1995) is adopted. Namely, in any quantity the left superscript indicates in which configuration the quantity occurs and the left subscript indicates the configuration with respect to which the quantity is measured. In a Total Lagrange (TL) formulation this subscript is equal to 0. Moreover, in this notation, a comma denotes differentiation with respect to the coordinate following.

The first step in linearizing the nonlinear equilibrium Eq. (1) is to decompose incrementally the stresses and the strains. The second Piola-Kirchhoff stresses $^{t+\Delta t}_0\mathbf{S}_{ij}$ are decomposed into

$$^{t+\Delta t}_0\mathbf{S}_{ij} = {}^t_0\mathbf{S}_{ij} + {}_0\mathbf{S}_{ij} \tag{4}$$

Similarly, the Green-Lagrange strains can be decomposed into

$$^{t+\Delta t}_0\varepsilon_{ij} = {}^t_0\varepsilon_{ij} + {}_0\varepsilon_{ij} \tag{5}$$

$$_0\varepsilon_{ij} = {}_0\mathbf{e}_{ij} + {}_0\mathbf{n}_{ij} \tag{6}$$

$$_0\mathbf{e}_{ij} = \frac{1}{2}({}_0\mathbf{u}_{i,j} + {}_0\mathbf{u}_{j,i} + \underbrace{{}^t_0\mathbf{u}_{k,i0}\mathbf{u}_{k,j} + {}_0\mathbf{u}_{k,i0}{}^t\mathbf{u}_{k,j}}_{\textit{Initial displacement effect}}) \tag{7}$$

$$_0\mathbf{n}_{ij} = \frac{1}{2}{}_0\mathbf{u}_{k,i0}\mathbf{u}_{k,j} \tag{8}$$

where $_0\mathbf{S}_{ij}$ are the incremental second Piola-Kirchhoff stress components and $_0\varepsilon_{ij}$ are the incremental Green-Lagrange strain components.

Next, the nonlinear equilibrium equations are formulated, taking into account the incremental decompositions of stresses and strains. Noting that $\delta^{t+\Delta t}_0\varepsilon_{ij} = \delta_0\varepsilon_{ij}$, the equilibrium equation is

$$\int_{^0V}{}_0\mathbf{S}_{ij}\delta_0\varepsilon_{ij}d^0V + \int_{^0V}{}^t_0\mathbf{S}_{ij}\delta_0\mathbf{n}_{ij}d^0V = {}^{t+\Delta t}\mathbf{R} - \int_{^0V}{}^t_0\mathbf{S}_{ij}\delta_0\mathbf{e}_{ij}d^0V \tag{9}$$

The final step is the linearization of Eq. (9). Using the approximations $_0\mathbf{S}_{ij} = {}_0\mathbf{C}_{ijrs}{}_0\mathbf{e}_{rs}$ and $\delta_0\varepsilon_{ij} = \delta_0\mathbf{e}_{ij}$ we obtain the following approximate equilibrium equation (see also Brendel and Ramm 1980)

$$\int_{^0V}{}_0\mathbf{C}_{ijrs}{}_0\mathbf{e}_{rs}\delta_0\mathbf{e}_{ij}d^0V + \int_{^0V}{}^t_0\mathbf{S}_{ij}\delta_0\mathbf{n}_{ij}d^0V = {}^{t+\Delta t}\mathbf{R} - \int_{^0V}{}^t_0\mathbf{S}_{ij}\delta_0\mathbf{e}_{ij}d^0V \tag{10}$$

where $_0\mathbf{C}_{ijrs}$ is the incremental stress-strain tensor at time t, referred to the configuration at time 0.

Eq. (10) is the well-known linearized equilibrium equation of the Total Lagrange (TL) formulation. The global stiffness matrix of the structure can be obtained with usual assembly

procedures, after a displacement field is introduced using a finite element discretization. According to Brendel and Ramm (1980), from the first integral of the left-hand side of Eq. (10), arise two stiffness matrices, namely the linear elastic matrix ${}_0^t\mathbf{K}_0$ and the initial displacement matrix ${}_0^t\mathbf{K}_u$ (due to the terms of the initial displacement effect of Eq. (7)). From the second integral of the left-hand side of Eq. (10), we get the initial stress or geometric matrix ${}_0^t\mathbf{K}_g$. Finally, the integral of the right-hand side of Eq. (10) gives rise to the vector of the internal forces in configuration t which are denoted as ${}_0^t\mathbf{F}$.

Thus, in the finite element method context, Eq. (10) can be written in a matrix form as

$$\left(\underbrace{{}_0^t\mathbf{K}_0 + {}_0^t\mathbf{K}_u + {}_0^t\mathbf{K}_g}_{{}_0^t\mathbf{K}} \right) \Delta\mathbf{U} = {}^{t+\Delta t}\mathbf{R} - {}_0^t\mathbf{F} \tag{11}$$

where ${}_0^t\mathbf{K}$ is the tangent stiffness of the structure and $\Delta\mathbf{U}$ is an increment to the current displacement vector.

3. Buckling analysis

At collapse or buckling of the structure, the tangent stiffness is singular. The condition of instability of the structure then reads as

$$\det({}_0^t\mathbf{K}) = \det({}_0^t\mathbf{K}_0 + {}_0^t\mathbf{K}_u + {}_0^t\mathbf{K}_g) = 0 \tag{12}$$

According to Brendel and Ramm (1980) and Tschope (2001), the following nonlinear buckling problems can be formulated

$$({}_0^t\mathbf{K}_0 + {}_0^t\mathbf{K}_u + {}^t\lambda\, {}_0^t\mathbf{K}_g)\phi_i = 0 \tag{13}$$

$$({}_0^t\mathbf{K}_0 + {}^t\lambda({}_0^t\mathbf{K}_u + {}_0^t\mathbf{K}_g))\phi_i = 0 \tag{14}$$

which differ from each other in the way that the load parameter ${}^t\lambda$ of the buckling load ${}^t\lambda\mathbf{R}$ is related to the elements of the tangent stiffness matrix. In the above equations ϕ_i denotes the ith buckling mode.

If the initial displacement matrix ${}_0^t\mathbf{K}_u$ is omitted from the two nonlinear buckling problems, then the classical buckling problem can be obtained

$$({}_0^t\mathbf{K}_0 + {}^t\lambda\, {}_0^t\mathbf{K}_g)\phi_i = 0 \tag{15}$$

4. Linearized buckling algorithms of ADINA and ABAQUS

ADINA has two buckling analysis formulations (ADINA 2006). The first formulation is called 'Secant' method and the second 'Classical' method. ABAQUS provides a choice of buckling analysis with or without nonlinear preloading. The buckling analysis algorithms of the two programs are briefly summarized next.

4.1 ADINA 'Secant' formulation

The basic equation of the 'Secant' formulation is the following

$$_0^{t_1}\mathbf{K}\phi_i = \gamma_i {}_0^{t_0}\mathbf{K}\phi_i \tag{16}$$

where $_0^{t_0}\mathbf{K}$ and $_0^{t_1}\mathbf{K}$ are the stiffness matrices at times t_0 and t_1 respectively, t_0 is the time at the beginning of the analysis, t_1 is equal to $t_0 + \Delta t$, where Δt is a time increment, ϕ_i is the ith eigenmode, and γ_i is a function of the eigenvalue λ_i

$$\gamma_i = 1 - \frac{1}{\lambda_i} \tag{17}$$

If we replace Eq. (17) in Eq. (16) we get

$$_0^{t_1}\mathbf{K}\phi_i = \gamma_i {}_0^{t_0}\mathbf{K}\phi_i \Rightarrow {}_0^{t_1}\mathbf{K}\phi_i = \left(1 - \frac{1}{\lambda_i}\right){}_0^{t_0}\mathbf{K}\phi_i \Rightarrow ({}_0^{t_1}\mathbf{K} - {}_0^{t_0}\mathbf{K})\phi_i + \frac{1}{\lambda_i}{}_0^{t_0}\mathbf{K}\phi_i = 0 \Rightarrow$$

$$({}_0^{t_0}\mathbf{K} + \lambda_i({}_0^{t_1}\mathbf{K} - {}_0^{t_0}\mathbf{K}))\phi_i = 0 \tag{18}$$

Taking a close look at Eq. (18), we can see that the 'Secant' formulation does not solve the classical buckling problem, since $_0^{t_0}\mathbf{K}$ is not the linear stiffness matrix, and $_0^{t_1}\mathbf{K} - {}_0^{t_0}\mathbf{K}$ does not correspond to the initial stress stiffness matrix $_0^{t_1}\mathbf{K}_g$.

In the 'Secant' buckling analysis, the critical loads $\mathbf{R}_{cr,i}$ are determined from the critical load factor using

$$\mathbf{R}_{cr,i} = {}^{t_0}\mathbf{R} + \lambda_i({}^{t_1}\mathbf{R} - {}^{t_0}\mathbf{R}) \tag{19}$$

where $^{t_0}\mathbf{R}$ and $^{t_1}\mathbf{R}$ are the externally applied load vectors at times t_0 and t_1, respectively. When time t_0 corresponds to the original unstressed configuration, the critical load is equal to

$$\mathbf{R}_{cr,i} = \lambda_i {}^{t_1}\mathbf{R} \tag{20}$$

$^{t_1}\mathbf{R}$ is considered as the reference load, which is used in the following numerical examples, and which has a major impact on the numerical results of both the buckling loads and the buckling modes.

4.2 ADINA 'Classical' formulation

The basic equation of the 'Classical' formulation is

$$_0^{t_1}\mathbf{K}\phi_i = \gamma_i({}_0^{t_1}\mathbf{K} - {}_0^{t_1}\mathbf{K}_g)\phi_i \Rightarrow {}_0^{t_1}\mathbf{K}\phi_i = \left(1 - \frac{1}{\lambda_i}\right)({}_0^{t_1}\mathbf{K} - {}_0^{t_1}\mathbf{K}_g)\phi_i \Rightarrow {}_0^{t_1}\mathbf{K}_g\phi_i = \frac{1}{\lambda_i}({}_0^{t_1}\mathbf{K}_g - {}_0^{t_1}\mathbf{K})\phi_i \Rightarrow$$

$$(({}_0^{t_1}\mathbf{K} - {}_0^{t_1}\mathbf{K}_g) + \lambda_i {}_0^{t_1}\mathbf{K}_g)\phi_i = 0 \Rightarrow ({}_0^{t_1}\mathbf{K}_0 + {}_0^{t_1}\mathbf{K}_u + \lambda_i {}_0^{t_1}\mathbf{K}_g)\phi_i = 0 \tag{21}$$

According to Section 3, it is concluded that the buckling problem of Eq. (21) does not correspond

to the classical buckling problem of Eq. (15), but to the nonlinear buckling problem of Eq. (13). When the applied loads $^{t_1}\mathbf{R}$ are sufficiently small, then the buckling load estimated from Eq. (21) is practically the classical buckling load (see also Brendel and Ramm 1980).

In the 'Classical' buckling analysis, the critical load is determined by the critical load factor using

$$\mathbf{R}_{cr,i} = \lambda_i^{t_1}\mathbf{R} \tag{22}$$

where $^{t_1}\mathbf{R}$ is the reference load or the load applied for the buckling analysis of the structure.

4.3 ABAQUS buckling formulation

According to ABAQUS (2008), the buckling analysis formulation of ABAQUS is used to estimate bifurcation loads of 'stiff' structures. This estimation of the critical loads is performed with the aid of a linear perturbation procedure on a configuration of the structure named the base state. This base state can be the original configuration of the structure or can be the last estimated configuration of a previous linear or nonlinear static analysis step with a preload $\overline{\mathbf{P}}$. If during this step the geometric nonlinearity is omitted, then the base state geometry is the original configuration of the body. If this is the case, then the loads obtained from ABAQUS are the classical buckling loads. In the ABAQUS buckling formulation two matrices must be evaluated; the base state stiffness and the differential stiffness. The base state stiffness is the sum of the hypoelastic tangent stiffness, the initial stress stiffness and the load stiffness. According to Belytschko *et al.* (2000), the load stiffness matrix relates the rate of the external nodal forces to the nodal velocities. This stiffness matrix is relevant only when there are follower loads in the analysis, namely loads that change with the configuration of the body. The differential stiffness consists of the sum of the initial stress stiffness due to the perturbation stresses and the load stiffness due to perturbation loads.

Excluding the load stiffness in the following, in the absence of preload or in the case of linear preload, the ABAQUS buckling formulation is identical to the classical buckling problem

$$({}_0^t\mathbf{K}_0 + \lambda_i {}_0^t\mathbf{K}_g)\phi_i = 0 \tag{23}$$

When during a preload geometrical nonlinearity is taken into account, the base stiffness matrix ${}_0^t\mathbf{K}_0$ is replaced by the tangent stiffness matrix due to the preload $\overline{\mathbf{P}}$, and the initial stress stiffness is replaced by the differential stiffness due to perturbation stresses and loads estimated from the base state of the structure.

Finally, the critical buckling loads are equal to $\overline{\mathbf{P}} + \lambda_i \mathbf{Q}$, where λ_i is the *i*th eigenvalue obtained from the buckling problem and $\mathbf{Q}$ is the incremental loading pattern in the eigenvalue buckling prediction step which is also considered as the reference load.

5. Examples

Three specific numerical examples are studied in this section using all buckling analysis formulations described above. In the first example a simply-supported column in compression is analyzed, typical of structures with linear pre-buckling behaviour and stable post-buckling path. The second example, of a shallow arch subjected to a concentrated load at the crown, is characteristic of

structures with nonlinear pre-buckling behaviour. The third example concerns a thin-walled cylindrical shell subjected to pure bending, and is typical of structures with linear pre-buckling behaviour and a sharp unstable post-buckling response.

5.1 Column under compression

Initially, the case of a simply-supported, 3 m long steel column with a hollow square cross-section of 200 mm width and 10 mm thickness is considered. An elastic constitutive material law with Young's modulus equal to 210 GPa is used for the steel. The classical buckling load is given by the well-known Euler formula

$$P_{cl} = \frac{\pi^2 EI}{L^2} \Rightarrow P_{cl} = \frac{\pi^2 \times 210 \text{ GPa} \times 4585.33 \text{ cm}^4}{(3.0 \text{ m})^2} = 10559.6 \text{ kN} \qquad (24)$$

After a convergence study it was found that 20 Hermitian beam elements for ADINA and 20 B33 2-node cubic beam elements of ABAQUS were sufficient for an accurate estimation of the Euler buckling load.

By performing a buckling analysis with ABAQUS with no preloading, a buckling load of 10530 kN is obtained, which is considered as a good approximation of the Euler buckling load. It is reminded that this analysis corresponds to the classical buckling problem. Then, the problem is also solved with both buckling formulations of ADINA, the 'Classical' and the 'Secant' formulation, as well as with ABAQUS with preloading. The first buckling mode obtained from all buckling formulations is practically the same, as shown in Fig. 1. The buckling mode has been evaluated for reference loads of 10 kN and 10000 kN and it was concluded that it remains the same without being affected by the magnitude of the reference load.

In Fig. 2 the eigenvalue function, which relates the buckling load P_{LBA} to the reference load P_{ref} (equal to preload in case of ABAQUS), both normalized with respect to the classical buckling P_{cl}, is plotted for the two buckling formulations of ADINA, as well as for the buckling formulation of
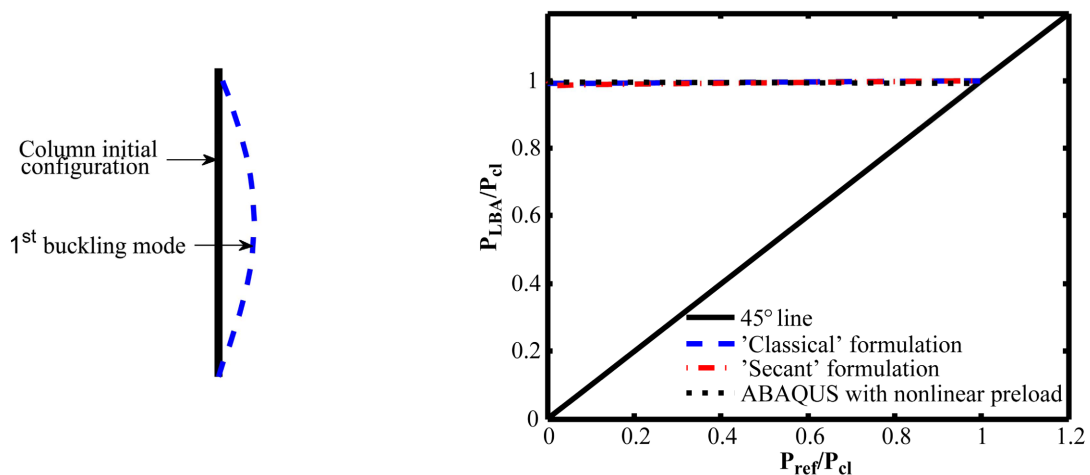

Fig. 1 First buckling mode obtained from all buckling formulations

Fig. 2 Eigenvalue function of column
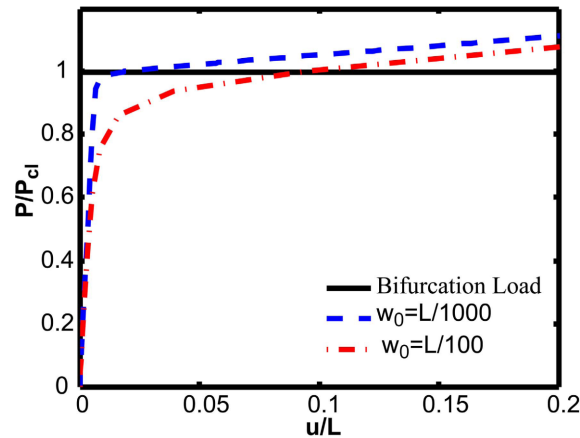
Fig. 3 Load-displacement curve of column from GNI analyses

ABAQUS taking into account nonlinear preloading. It is observed that the buckling load is practically independent from the magnitude of the reference load for all buckling formulations. The constant nature of the eigenvalue function can be contributed to the fact that no significant nonlinear effects appear in the column before buckling.

This is verified in Fig. 3, where load-displacement curves from a Geometrically Nonlinear Analysis with Imperfections (GNIA), obtained using ADINA, are given. As an imperfection, the first buckling mode is considered in the analyses, with amplitude w_0 equal to a fraction of the column length L. On the horizontal axis the axial displacement u of the loaded edge is normalized with respect to the length of the column L. On the vertical axis the applied load P is normalized with respect to the classical buckling load P_{cl}. The linear nature of the pre-buckling response for small imperfection magnitudes is verified. Column buckling is demonstrated as the applied load approaches P_{cl}, by the sharp decrease in stiffness, triggered by the imperfection. As imperfection amplitudes become larger, buckling is initiated at smaller loads and stiffness degradation becomes smoother.

One interesting property of the eigenvalue function is the fact that it does not intersect the 45º line. This holds for the two buckling formulations of ADINA and the buckling analysis of ABAQUS with nonlinear preloading. This is because all algorithms require that the reference load is not larger than the buckling load, otherwise no convergence is possible.

It should be stated here, that in the case of ABAQUS buckling algorithm with nonlinear preloading, for an extremely small range of values for the preload magnitude ($10456 \, \text{kN} \leq \overline{P} \leq 10460 \, \text{kN}$), it was found that the algorithm estimated the second buckling mode of the column. For larger values of the preload magnitude ($\overline{P} > 10460 \, \text{kN}$), the analysis was terminated with an error message that the model is probably loaded above the bifurcation (buckling) load.

5.2 Circular arch under concentrated load at the crown

The second example is that of a circular steel arch with radius $R = 50$ m, height $H = 1.7037$ m, span $L = 25.882$ m, length $S = 26.18$ m and subtended angle $\theta = 30º$. An elastic constitutive material law with Young's modulus equal to 210 GPa is used for the steel. The arch is loaded with a concentrated load P at the crown (Fig. 4).
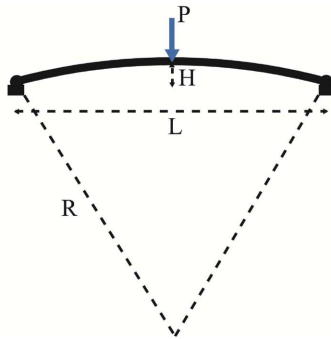
Fig. 4 Geometry and loading of arch
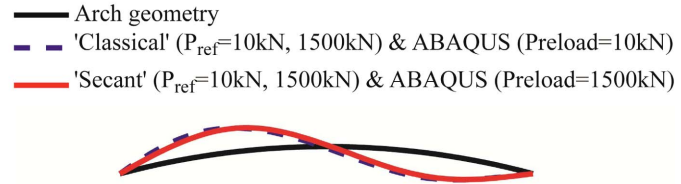
Fig. 5 Buckling mode of arch from all buckling formulations

The problem is solved numerically with both finite element programs, ADINA and ABAQUS. Firstly, a convergence study was carried out, in order to find a sufficient mesh for estimating the buckling loads. It was found that 100 Hermitian beam elements and 100 B31 2-node linear beams are sufficiently accurate for the subsequent calculations.

In ABAQUS the buckling load that is calculated, if no nonlinear effects are taken into account at the base state due to preload, does not depend on the reference load so it can be considered as the classical buckling load. For the arch under investigation, this buckling load, calculated with ABAQUS, is equal to

$$P_{ABAQUS} = P_{cl} = 1893.3 \text{ kN} \tag{25}$$

In Fig. 5, the first buckling mode is shown for the three buckling formulations for two reference loads or preloads. As the reference load increases from 10 kN to 1500 kN there are no significant changes in the shape of the buckling mode for 'Classical' and 'Secant' formulations. However, there is a slight difference between the buckling modes of the two formulations although the type remains the same, namely asymmetric. On the other hand, for preload of 10 kN the ABAQUS buckling formulation gives a buckling mode that is very close to the corresponding mode of 'Classical' formulation. For preload of 1500 kN the buckling mode of ABAQUS is now very close to the buckling mode of 'Secant' formulation. This can be explained by the eigenvalue function for the arch problem given below. For low reference loads, the ABAQUS buckling formulation is closer to the 'Classical' formulation. However, as the reference load or the preload increases the ABAQUS buckling formulation approaches the 'Secant' formulation.

This buckling mode is taken into account in GNI analyses for a number of imperfection amplitudes, in order to study the imperfection sensitivity of the arch (Fig. 6). When no imperfection is considered in the analysis (GN analysis), then the arch fails through a limit point. The maximum load in this case is

$$P_{GNA} = 1795.82 \text{ kN} \tag{26}$$

When a small antisymmetric imperfection ($w_0 = S/1000000$) with the shape of the first buckling mode is introduced, the arch fails through a bifurcation point

$$P_{GNIA} = 1621.86 \text{ kN} \tag{27}$$

In Fig. 7 the deformed configurations at different characteristic positions at the load-displacement
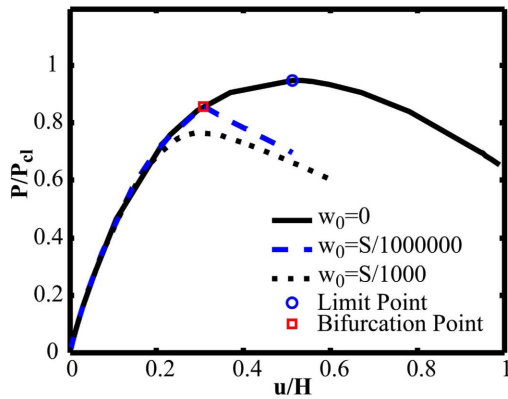
Fig. 6 Load-displacement curve of arch from GNI analyses
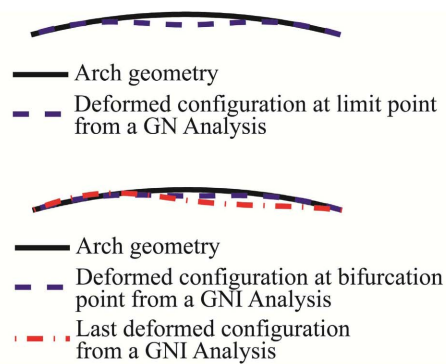
Fig. 7 Deformed configurations of arch from GNI analyses
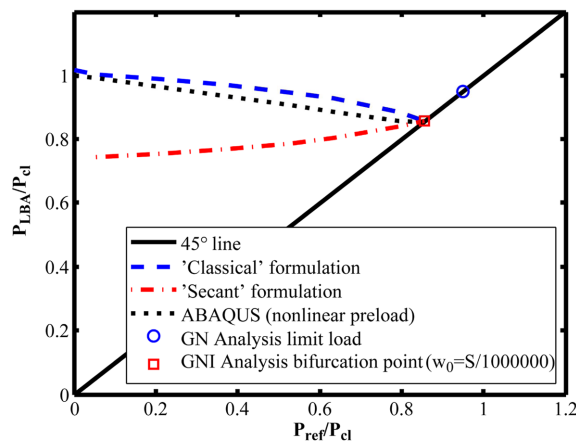
Fig. 8 Eigenvalue function of arch for all buckling formulations

curves of Fig. 6 are given. These configurations concern both the limit point of the GN analysis and the bifurcation point of the GNI analysis. In the second case the last estimated configuration is also given. When no imperfection is taken into account, the deformation up to the limit point is symmetric. When a very small imperfection of magnitude $S/1000000$ is considered, the deformation up to the bifurcation point is practically symmetrical. After bifurcation takes place, asymmetric deformation appears.

In Fig. 8, the eigenvalue functions for all buckling formulations are plotted. It can be seen that for small values of the reference load the buckling load obtained from the Classical' formulation of ADINA and from ABAQUS with nonlinear preloading provide good approximations of the classical buckling load. These two eigenvalue functions exhibit similar characteristics. As the reference load increases the buckling load decreases. On the other hand, ADINA's 'Secant' formulation underestimates the classical buckling load for small values of the reference load, and increases for increasing reference load. It is very interesting to observe that all three buckling formulations intersect the 45-degree line at a value that is practically equal to the bifurcation point of a GNI

analysis, in other words they can actually predict the nonlinear elastic failure load of the arch.

5.3 Cylindrical shell under pure bending

The third example concerns a cylindrical steel shell with length $L = 14$ m, diameter $D = 3$ m and thickness $t = 20$ mm. An elastic constitutive material law with Young's modulus equal to 210 GPa is used for the steel. The shell is subjected to a bending moment at the one edge. One edge of the shell is clamped and at the other edge the displacement degree of freedom in the direction of the bending moment and the rotational degree of freedom in the direction of the axis of the shell are fixed (Fig. 9).

The problem is solved numerically with both finite element programs, ADINA and ABAQUS. First, a convergence study is performed in order to obtain an efficient finite element mesh for predicting the buckling load. It was found that 9243 MITC4 shell elements in ADINA and the same number of S4 shell finite elements in ABAQUS are sufficient.

The buckling load obtained from a buckling analysis with ABAQUS with no preload can be considered as the classical buckling load

$$M_{ABAQUS} = M_{cl} = 259775 \text{ kNm} \tag{28}$$

In Fig. 10, the first buckling mode is shown, as obtained from the 'Classical' buckling formulation of ADINA with $M_{ref} = 2597.74$ kNm.

This imperfection is taken into account in GNI analyses in order to study the imperfection sensitivity of the shell under bending. In Fig. 11 the moment-rotation curves from these analyses are plotted. In the vertical axis the applied moment is normalized with respect to M_{cl}. In the horizontal axis the rotation of the node on which the concentrated moment is applied is given.

From Fig. 11 it is verified that the shell is very imperfection sensitive. For example, if an imperfection with magnitude $t/10$ is applied, then the buckling load of the imperfect shell is almost 47% smaller than the buckling load of the perfect shell.

The collapse load obtained from GN analysis with ADINA is equal to

$$M_{GNA} = 214271 \text{ kNm} \tag{29}$$

In Fig. 12 the first buckling mode obtained from the three studied buckling formulations for two different reference load levels in the case of ADINA or corresponding magnitudes of preloading $\overline{M}$
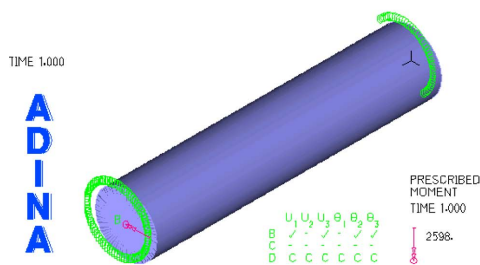

Fig. 9 Cylindrical shell under bending
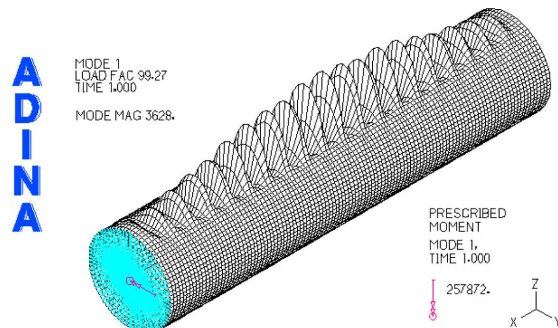
Fig. 10 First buckling mode of cylindrical shell from 'Classical' buckling formulation of ADINA
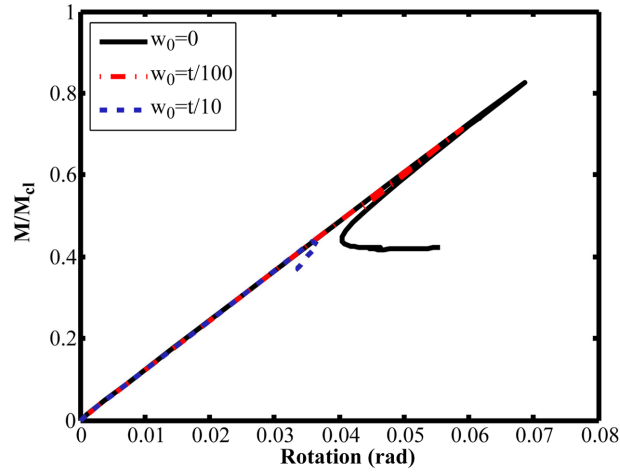
Fig. 11 Moment-rotation curve of cylindrical shell from GNI analyses

	M_{ref} (ADINA) or $\bar{M}$(ABAQUS) in kNm	
	10000	200000
ADINA 'Classical'		
ADINA 'Secant'		
ABAQUS (nonlinear preloading)		
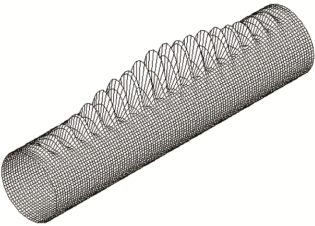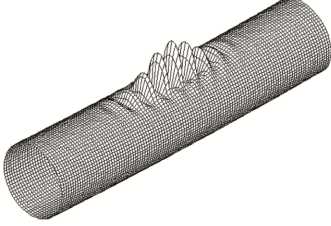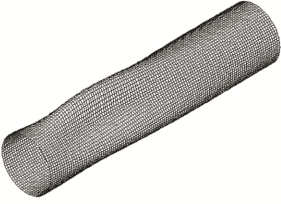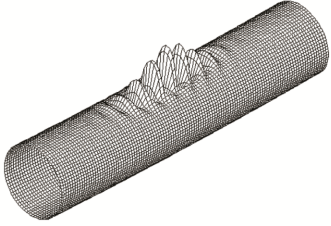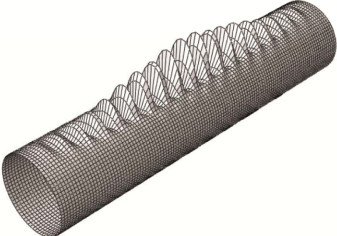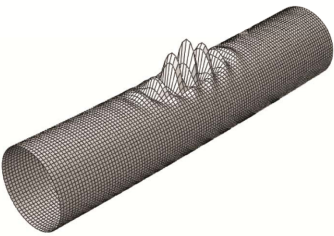
Fig. 12 First buckling mode with respect to the reference load
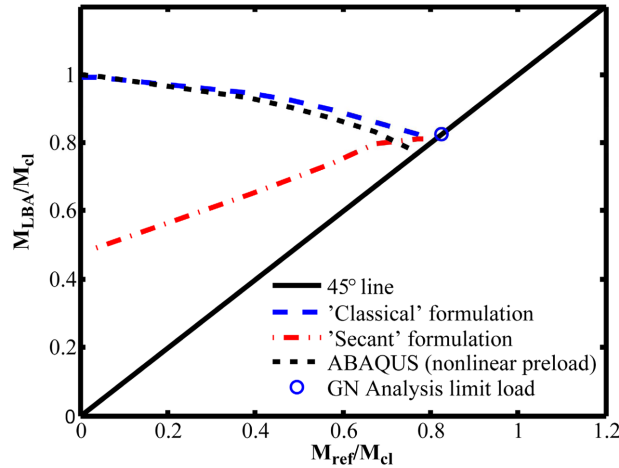
Fig. 13 Eigenvalue function of cylindrical shell under bending

in the case of ABAQUS are given. It is observed that there is a very good agreement between the 'Classical' buckling formulation of ADINA and the buckling formulation of ABAQUS with nonlinear preloading. For the higher reference load of 200000 kNm, 'Secant' buckling algorithms agrees well with the two other buckling formulations. On the other hand, for the low level of reference load of 10000 kNm, the buckling mode of 'Secant' formulation departs significantly from the corresponding buckling mode of the other two formulations.

In Fig. 13 the eigenvalue functions of the three algorithms for the cylindrical shell under bending are plotted. If the reference load is kept to low levels, ADINA's 'Classical' formulation gives a good approximation of the classical buckling load. Another important observation is that both ADINA formulations lead to the same buckling load as the reference load is gradually increased up to the value of 203500 kNm. If this reference load is used the calculated buckling load is equal to 213038 kNm and 210775 kNm for the 'Classical' and 'Secant' buckling formulations, respectively. These nonlinear buckling loads are very good approximations of the nonlinear collapse load, which is equal to 214271 kNm, as obtained by a GN analysis with the *Collapse Analysis* algorithm of ADINA (Bathe and Dvorkin 1983). Comparing the eigenvalue function of the ABAQUS buckling algorithm with nonlinear preloading it can be seen that it resembles with the results of the 'Classical' buckling formulation of ADINA, but it eventually leads to a slightly smaller buckling load at the intersection with the 45° line. It is also interesting to note that the significant difference of 'Secant' formulation at low levels of reference load with respect to the other two formulations, can be contributed to the different buckling modes that it calculates (see Fig. 12).

6. Conclusions

Linear buckling analyses are important tools for practical structural design. Experience from buckling analyses performed with commercial finite element software has shown that the shape of buckling modes and the magnitude of buckling loads may differ, sometimes significantly, from one algorithm to another, and may depend on the magnitude of the reference load. Three examples have

been used in order to assess the linear buckling formulations available in the well known finite element programs ADINA and ABAQUS. The first example, of a simply-supported column in compression, is typical of structures that have a linear pre-buckling behaviour and a stable post-buckling path. The second example, of a shallow arch subjected to a concentrated load at the crown, is characteristic of structures with nonlinear pre-buckling behaviour. The third example, of a thin-walled cylindrical shell subjected to pure bending, is typical of structures with linear pre-buckling behaviour and a sharp unstable post-buckling response.

Among the buckling algorithms that have been studied, the only one corresponding to the classical buckling analysis is the formulation of ABAQUS without preloading. The 'Classical' formulation of ADINA and the formulation of ABAQUS with nonlinear preloading yield a good approximation of the classical buckling load for sufficiently small reference loads. A practical way of determining such low levels of the reference load is to perform first a buckling analysis with a random reference load to get a first estimation of the buckling load, and then use 1/100 of this buckling load as a reference load in a second buckling analysis. ADINA's 'Secant' formulation does not lead to acceptable approximations of the classical buckling load.

Both buckling formulations of ADINA as well as the formulation of ABAQUS with nonlinear preloading provide good approximations of the actual geometrically nonlinear buckling loads, if the reference load is close to the eventual buckling load. This can be achieved by performing successive buckling analyses, gradually increasing the reference load, and plotting the eigenvalue functions until they intersect the 45° line. In this process, the two buckling formulations of ADINA proved more accurate than the buckling formulation of ABAQUS with nonlinear preloading.

The above conclusions are useful for guiding engineers using linear buckling analysis for one of the four reasons mentioned above, in selecting the appropriate software and algorithm and in evaluating the results. Moreover, the three examples presented in this paper may be used as benchmark problems when employing other finite element software for linear buckling analysis in the framework of practical structural steel design.

References

ABAQUS/Standard and ABAQUS/Explicit - Version 6.8 (2008), *Abaqus Theory Manual*, Dassault Systems.

ADINA R & D Inc. (2006), *Theory and Modeling Guide Volume I: ADINA*, Report ARD 06-7.

Agüero, A. and Pallarés, F.J. (2007), "Proposal to evaluate the ultimate limit state of slender structures. Part 1: Technical aspects", *Eng. Struct.*, **29**(4), 483-497.

Al-Bermani, F.G.A. and Kitipornchai, S. (1990), "Elastoplastic large deformation analysis of thin walled structures", *Eng. Struct.*, **12**(1), 28-36.

Al-Bermani, F.G.A. and Kitipornchai, S. (1992), "Nonlinear analysis of transmission towers", *Eng. Struct.*, **14**(3), 139-151.

American Institute of Steel Construction (1999), *Load and Resistance Factor Design for Structural Steel Buildings*.

Baldassino, N. and Bernuzzi, C. (2000), "Analysis and behaviour of steel storage pallet racks", *Thin Wall. Struct.*, **37**(4), 277-304.

Bathe, K.J. and Cimento, A.P. (1980), "Some practical procedures for the solution of nonlinear finite element equations", *Comput. Meth. Appl. Mech. Eng.*, **22**(1), 59-85.

Bathe, K.J., Snyder, M.D., Cimento, A.P. and Rolph, W.D. (1980), "On some current procedures and difficulties in finite element analysis of elastic-plastic response", *Comput. Struct.*, **12**(4), 607-624.

Bathe, K.J. and Dvorkin, E.N. (1983), "On the automatic solution of nonlinear finite element equations",

Comput. Struct., **17**, 871-879.

Bathe, K.J. (1995), *Finite Element Procedures*, Prentice-Hall, Englewood Cliffs.

Belytschko, T., Liu, W.K. and Moran, B. (2000), *Nonlinear Finite Elements for Continua and Structures*, John Wiley & Sons Ltd.

Berry, P.A., Rotter, J.M. and Bridge, R.Q. (2000), "Compression tests on cylinders with circumferential weld depressions", *J. Eng. Mech., ASCE*, **126**(4), 405-413.

Brendel, B. and Ramm, E. (1980), "Linear and nonlinear stability analysis of cylindrical shells", *Comput. Struct.*, **12**, 549-558.

Chan, S.L. (1989), "Inelastic post-buckling analysis of tubular beam-columns and frames", *Eng. Struct.*, **11**(1), 23-30.

Chan, S.L. and Chui, P.T. (2000), *Non-linear Static and Cyclic Analysis of Semirigid Steel Frames,* Elsevier Science, Amsterdam.

Chang, S.C. and Chen, J.J. (1986), "Effectiveness of linear bifurcation analysis for predicting the nonlinear stability limits of structures", *Int. J. Numer. Meth. Eng.*, **23**, 831-846.

Chen, W.F. and Kim, S.E. (1997), *LRFD Steel Design Using Advanced Analysis*, CRC Press, Boca Raton, Florida.

Crisfield, M.A. (1981), "A fast incremental/iterative solution procedure that handles snap-through", *Comput. Struct.*, **13**, 55-62.

Crisfield, M.A., Jelenic, G., Mi, Y., Zhong, H.G. and Fan, Z. (1997), "Some aspects of the non-linear finite element method", *Finite Elem. Anal. Des.*, **27**(1), 19-40.

Dimopoulos, C.A. and Gantes, C.J. (2008a), "Design of circular steel arches with hollow circular cross-sections according to EC3", *J. Constr. Steel Res.,* **64**(10), 1077-1085.

Dimopoulos, C.A. and Gantes, C.J. (2008b), "Nonlinear in-plane behavior of circular steel arches with hollow circular cross-section", *J. Constr. Steel Res.,* **64**(12), 1436-1445.

Earls C.J. (2007), "Observations on eigenvalue buckling analysis within a finite element context", *Proceedings of the Structural Stability Research Council*, Annual Stability Conference, New Orleans, LA, USA.

Elgaaly, M. (2000), "Post-buckling behaviour of thin steel plates using computational models", *Adv. Eng. Softw.*, **31**(8-9), 511-517.

European Committee for Standardization (2004a), *Eurocode 3 – Design of Steel Structures – Part 1-1: General Rules and Rules for Buildings*.

European Committee for Standardization (2004b), *Eurocode 3 – Design of Steel Structures – Part 1.5: Plated Structural Elements*.

European Committee for Standardization (2006), *Eurocode 3 – Design of Steel Structures – Part 1.6: Strength and Stability of Shell Structures*.

Feng, M., Wang, Y.C. and Davies, J.M. (2004), "A numerical imperfection sensitivity study of cold-formed thin-walled tubular steel columns at uniform elevated temperatures", *Thin Wall. Struct.*, **42**, 533-555.

Gantes, C.J. and Fragkopoulos, K.A. (2010), "Strategy for numerical verification of steel structures at the ultimate limit state", *Struct. Infrastr. Eng.*, **6**(1-2).

Gettel, M. and Schneider, W. (2007), "Buckling strength verification of cantilevered cylindrical shells subjected to transverse load using Eurocode 3", *J. Constr. Steel Res.*, **63**(11), 1467-1478.

Hawileh, R.A., Abed, F., Abu-Obeidah, A.S. and Abdalla, J.A. (2012), "Experimental investigation of inelastic buckling of built-up steel columns", *Steel Compos. Struct.*, **13**(3).

Herynk, M.D., Kyriakides, S., Onoufriou, A. and Yun, H.D. (2007), "Effects of the UOE/UOC pipe manufacturing processes on pipe collapse pressure", *Int. J. Mech. Sci.*, **49**, 533-553.

Hsieh, S.H. and Deierlein, G.G. (1991), "Nonlinear analysis of three-dimensional steel frames with semi-rigid connections", *Comput. Struct.*, **41**(5), 995-1009.

Johansson, B., Maquoi, R. and Sedlacek, G. (2001), "New design rules for plated structures in Eurocode 3", *J. Constr. Steel Res.*, **57**(3), 279-311.

Kaitila, O. (2002), "Imperfection sensitivity analysis of lipped channel columns at high temperatures", *J. Constr. Steel Res.,* **58**, 333-351.

Kato, S., Mutoh, I. and Shomura, M. (1998), "Collapse of semi-rigidly jointed reticulated domes with initial geometric imperfections", *J. Constr. Steel Res.*, **48**(2-3), 145-167.

Kim, S.E., Park, M.H. and Choi, S.H. (2001), "Direct design of three-dimensional frames using practical advanced analysis", *Eng. Struct.*, **23**(11), 1491-1502.

Kojic, M. and Bathe, K.J. (2004), *Inelastic Analysis of Solids and Structures*, Series in Computational Fluid and Solid Mechanics, Springer Verlag, Berlin.

Liew, J.Y.R., White, D.W. and Chen, W.F. (1993), "Limit states design of semi-rigid frames using advanced analysis: part 2: analysis and design", *J. Constr. Steel Res.*, **26**(1), 29-57.

Liew, J.Y.R., Chen, W.F. and Chen, H. (2000), "Advanced inelastic analysis of frame structures", *J. Constr. Steel Res.*, **55**(1-3), 245-265.

Lignos, D.G., Krawinkler, H. and Whittaker A.S. (2011), "Prediction and validation of sidesway collapse of two scale models of a 4-story steel moment frame", *Earthq. Eng. Struct. D.*, **40**, 807-825.

Paik, J.K. and Thayamballi, A.K. (2003), *Ultimate Limit State Design of Steel-plated Structures*, Wiley, New Jersey.

Pi, Y.L. and Trahair, N.S. (1994a), "Nonlinear inelastic analysis of steel beam columns-theory", *J. Struct. Eng.*, ASCE, **120**(7), 2041-2061.

Pi, Y.L. and Trahair, N.S. (1994b), "Nonlinear inelastic analysis of steel beam columns-applications", *J. Struct. Eng.*, ASCE, **120**(7), 2062-2085.

Pi, Y.L. and Trahair, N.S. (1998), "Out-of-plane inelastic buckling and strength of steel arches", *J. Struct. Eng.*, ASCE, **124**(2), 174-183.

Pi, Y.L., Put, B.M. and Trahair, N.S. (1999), "Lateral buckling strengths of cold-formed Z-section beams", *Thin Wall. Struct.*, **34**(1), 65-93.

Pi, Y.L. and Bradford, M.A. (2004), "In-plane strength and design of fixed steel I-section arches", *Eng. Struct.*, **26**(3), 291-301.

Ramm, E. (1981), "Strategies for tracing nonlinear responses near limit points", *Nonlinear Finite Element Analysis in Structural Mechanics* (Eds. W. Wunderlich, E. Stein and K.J. Bathe), Springer-Verlag, New York.

Riks, E. (1979), "An incremental approach to the solution of snapping and buckling problems", *Int. J. Solids Struct.*, **15**, 529-551.

Rodrigues, P.F.N. and Jacob, B.P. (2005), "Collapse analysis of steel jacket structures for offshore oil exploitation", *J. Constr. Steel Res.*, **61**(8), 1147-1171.

Schneider, W. and Brede, A. (2005), "Consistent equivalent geometric imperfections for the numerical buckling strength verification of cylindrical shells under uniform external pressure", *Thin Wall. Struct.*, **43**(2), 175-188.

Schneider, W., Timmel, I. and Höhn, K. (2005), "The conception of quasi-collapse-affine imperfections: A new approach to unfavourable imperfections of thin-walled shell structures", *Thin Wall. Struct.*, **43**(8), 1202-1224.

Sedlacek, G. and Müller, C. (2006), "The European standard family and its basis", *J. Constr. Steel Res.*, **62**(11), 1047-1059.

Shanmugam, N.E., Liew, J.Y.R. and Lee, S.L. (1993), "Ultimate strength design of biaxially loaded steel box beam-columns", *J. Constr. Steel Res.*, **26**(2-3), 99-123.

Shi, G., Liu, Z., Ban, H.Y., Zhang, Y., Shi, Y.J. and Wang, Y.Q. (2012), "Tests and finite element analysis on the local buckling of 420 MPa steel equal angle columns under axial compression", *Steel Compos. Struct.*, **12**(1), 31-51.

Trahair, N.S. and Chan, S.L. (2003), "Out-of-plane advanced analysis of steel structures", *Eng. Struct.*, **25**(13), 1627-1637.

Tschope, H., Onate, E. and Wriggers, P. (2001), *Direct Computation of Instability Points with Inequality Constraints Using the Finite Element Method*, International Centre for Numerical Methods in Engineering, Barcelona.

Vila Real, P.M.M., Cazeli, R., Simões da Silva, L., Santiago, A. and Piloto, P. (2004), The effect of residual stresses in the lateral-torsional buckling of steel I-beams at elevated temperature, *J. Constr. Steel Res.*, **60**, 783-793.

White, D.W. (1993), "Plastic-hinge methods for advanced analysis of steel frames", *J. Constr. Steel Res.*, **24**(2), 121-152.

White, D.W. and Hajjar, J.F. (2000), "Stability of steel frames: the cases for simple elastic and rigorous inelastic analysis/design procedures", *Eng. Struct.*, **22**(5), 155-167.

Wriggers, P., Wagner, W. and Miehe, C. (1987), "A quadratically convergent procedure for the calculation of

stability points in finite element analysis", *Comput. Meth. Appl. Mech. Eng.*, **70**, 329-347.

Wriggers, P. and Simo, J.C. (1990), "A general procedure for the direct computation of turning and bifurcation points", *Int. J. Numer. Meth. Eng.*, **30**, 155-176.

Yang, Y.B., Yang, C.T., Chang, T.P. and Chang, P.K. (1997), "Effects of member buckling and yielding on ultimate strengths of space trusses", *Eng. Struct.*, **19**(2), 179-191.